Journal of Supramolecular Structure 5:1–14 (1976)

Hexagonal Packing of Lipid Acyl Chains and Membrane Plasticity

D. L. Dorset*, S. W. Hui§, and C. M. Strozewski*§

*Molecular Biophysics Department, Medical Foundation of Buffalo, New York 14203

§Biophysics Department, Roswell Park Memorial Institute, Buffalo, New York 14263

Electron microscope and electron diffraction observations on microcrystals of pure lipids (a phosphatidylethanolamine, two phosphatidylcholines, a phosphatidic acid, and a galactocerebroside) reveal an extreme flexibility of lipid layers when the acyl chains are hexagonally packed (d_{100} = 4.17 Å). This is corroborated by similar observations on wet bilayers of a lecithin. It is shown that more "crystalline" polymethylene packings do not impart such plasticity to lipid layers and are therefore an unsuitable structural matrix for dynamic biological membranes.

Key words: membrane structure, phospholipid, electron microscopy, electron diffraction

INTRODUCTION

The nature of lipid aliphatic chain lateral packing in biological membrane surfaces is a subject of current controversy. Early electron diffraction studies on dry membrane preparations (1, 2) indicated that the long acyl chains are crystallized into a $0_\perp$ methylene subcell (Fig. 1), a position which is still held by more recent work (3) on a membrane supposedly unaffected by drying. Other electron diffraction studies on single, wet phospholipid bilayers (4–7) and wet, unfixed, unstained single membranes (8, 9), however, argue in favor of a hexagonal packing of the lipid chains (Fig. 2) below the transition temperature, in agreement with results obtained from X-ray diffraction experiments (10).

Whereas the $0_\perp$ methylene subcell packing has been found in some phospholipid single crystals (as well as a new orthorhombic subcell related to it) (11, 12), the existence of the hexagonal subcell seems more universal in single crystals of these compounds (12, 13). Because of the different mechanical properties that may be imparted to a lipid layer, it is of interest to characterize the consequences of a particular methylene subcell packing for membrane plasticity (14, 15). As is described below, this can be done in an examination of various microcrystalline long-chain compounds by electron diffraction and electron microscopy.

Received, December 11, 1975; Accepted, March 11, 1976

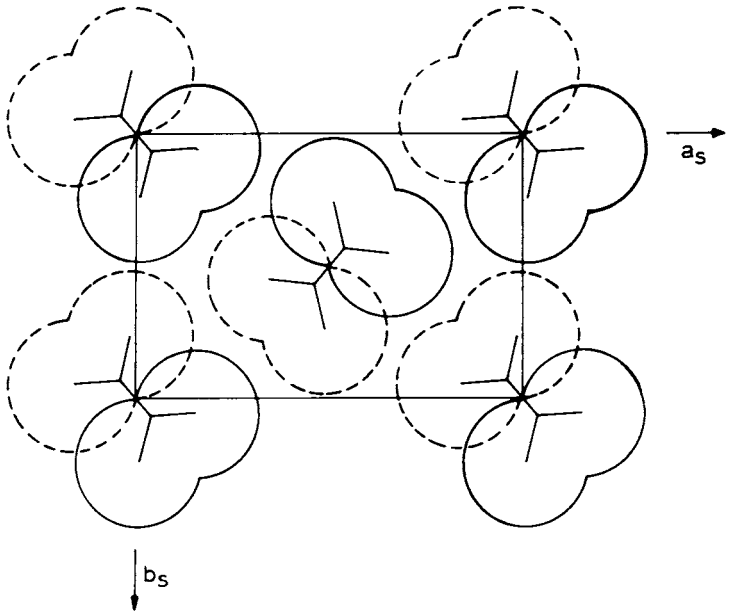

Fig. 1. Orthorhombic perpendicular ($0_\perp$) methylene subcell. View is down alkane chain axes corresponding to (001) projection of orthorhombic paraffins (20, 22). To produce polymethylene packing as found in, e.g., crystalline monoclinic paraffins, cetyl palmitate and the B-form of fatty acids (21), the chain axes are rotated ca. 27° around the subcell a $\simeq$ 7.5 Å axis (i.e., chain tilt to methyl end plane of about 60°). To produce polymethylene packing as found in, e.g., the crystalline C-form of fatty acids (29), the chain axes are rotated ca. 38° around the subcell a $\simeq$ 5.0 Å axis (i.e., chain tilt to methyl end plane about 50°).

METHODS

Lipid and Membrane Preparation

Microcrystals of the lipids listed below (99% pure, Serdary Research Labs, Inc., London, Ontario) were formed on 400-mesh electron microscope grids by rapid evaporation of dilute solutions in either absolute alcohol or chloroform. Grids covered with Formvar-carbon were used for the alcoholic solutions and carbon-film covered grids for the chloroform solutions.

Lipid		Solvent
sn-glycero-phosphoryl-ethanolamine, 1, 2-dihexadecyl ether	(DHPE)	EtOH
1, 2-distearoyl-sn-glycero-phosphoryl-choline	(DSPC)	EtOH
1, 2-dipalmitoyl-rac-glycero phosphoryl-choline	(DPPC)	EtOH
1, 2-dipalmitoyl-rac-glycero-phosphate	(DPPA)	EtOH
N-palmitoyl-dihydrogalactocere-broside	(NPGC)	$CHCl_3$

Bilayers were formed from synthetic 1, 2-dipalmitoyl-sn-glycero-phosphoryl choline (L-DPPC) (16) on 1,000-mesh copper electron microscope grids as described earlier (4).

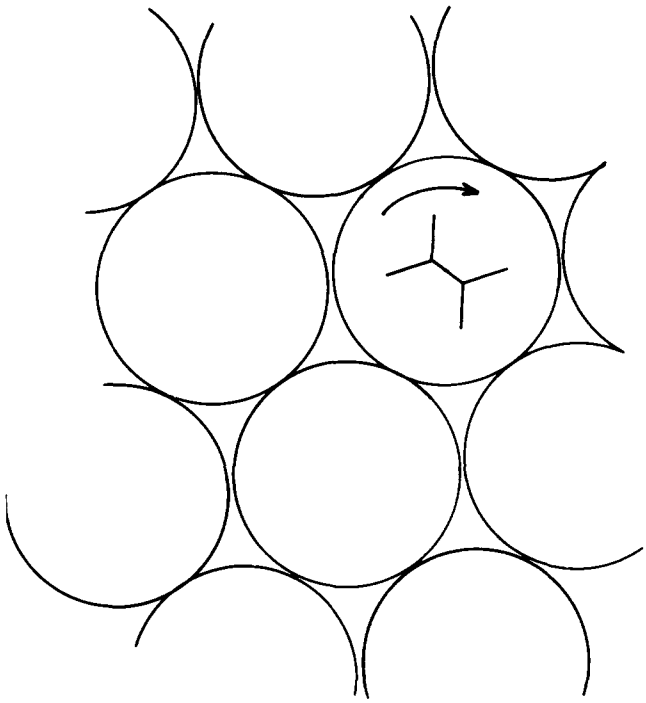

Fig. 2. Hexagonal methylene subcell. View is again down the alkane chain axes. Although the chains are probably helically twisted and undergoing thermal librations, the mathematical model for the diffraction intensities (33) in this (001) projection in space average is identical to a free methylene rotor as indicated (see Ref. 13 for further discussion). This subcell is a stable premelt acyl chain packing for many crystalline lipids.

Electron Microscopy and Diffraction

Electron diffraction experiments on lipid microcrystals were carried out by operating JEOL JEM-100U and JEM-100C electron microscopes at 100 kV and in the selected area diffraction mode. As described in earlier publications (13, 17) protective precautions against radiation damage were made. Diffraction spacings were calibrated with an internal gold powder diffraction standard. A Joyce-Loebl MkIIIC flat-bed microdensitometer was used to measure intensities from the diffraction films. Electron microscopy of gold-shadowed crystals was performed with a Siemens I A electron microscope operated at 80 kV.

Electron diffraction and dark-field microscopy of wet phospholipid bilayers are made possible with the differentially pumped wet specimen chamber described (18) for the Siemens IA electron microscope used for these experiments. The microscope was operated at 100 kV, and adequate precautions were taken again to protect the specimens against radiation damage. Diffraction spacings were calibrated with an internal aluminum powder diffraction standard.

RESULTS

sn-Glycero-phosphoryl-ethanolamine, 1, 2-dihexadecyl ether (DHPE)

Single crystals of the cephalin diacyl ether grow around a screw dislocation (Fig. 3) and are very easily deformed by forces imposed by rapid evaporation of solvent during

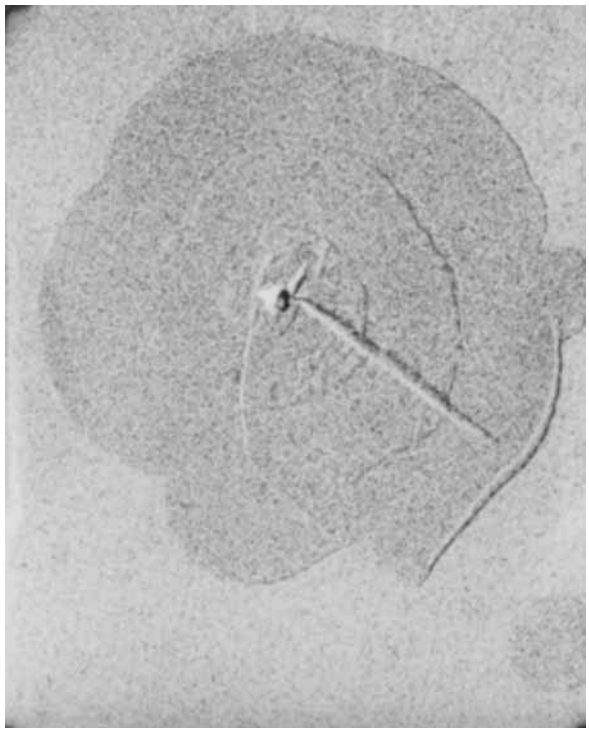

Fig. 3. Virtually undistorted single crystal of sn-glycero-phosphoryl-ethanolamine, 1, 2-dihexadecyl ether showing growth around screw dislocation. Graininess is due to coarse gold shadowing.

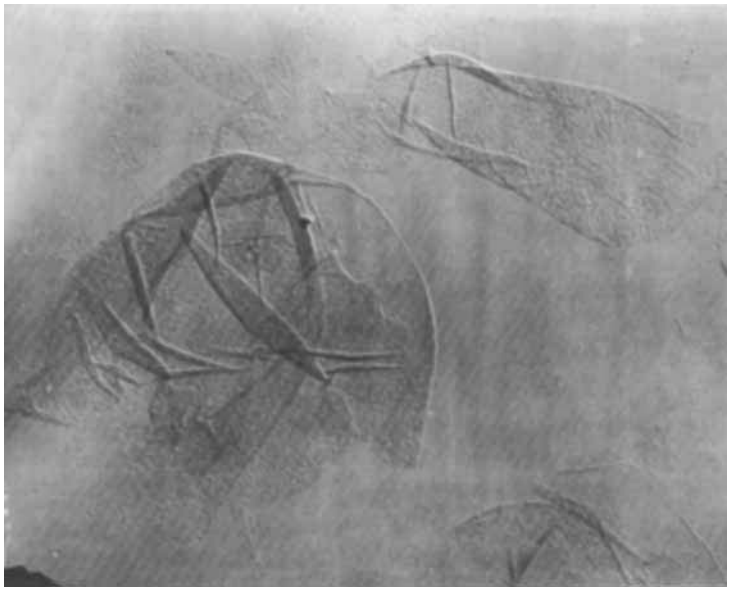

Fig. 4. Distorted (gold-shadowed) single crystals of sn-glycero-phosphoryl-ethanolamine, 1, 2-dihexadecyl ether showing elastic folds.

the crystallization process (Fig. 4). Careful examination of the deformed crystals are also seen to reveal an ill-defined dendritic overgrowth which, when magnified (Fig. 5), give branchings of the dendritic tree clustered around the values 68° and 60°.

Hexagonal diffraction patterns obtained with a large selected area (ca. 14 μm diam.) most usually resemble Fig. 6 and originate from the crystal habit shown above. The spacings of the most intense hexads are: 4.68 ± 0.02 Å, 4.17 ± 0.02 Å and 3.87 ± 0.02 Å. Use of smaller selected area apertures (ca. 0.3 μm diam.) gives diffraction patterns as shown in Fig. 7. It is seen that there is only one true hexagonal component with (100) spacing: 4.17 Å – undoubtedly corresponding to the often observed high-temperature form of long chain lipids (19), since the calculated intensity data of a rigid methylene rotor (see Fig. 2) (13, 17) agree very well with the observed intensities (Table I). This acyl packing is associated with the underlying DHPE bilayer and apparently posits the epitaxy responsible for the other diffraction spacings.

Occasionally two other crystal forms of DHPE are seen, both crystallizing in the well-known $0_{\perp}$ methylene subcell, one with chain axes normal to the crystal surface as in the case of orthorhombic n-paraffins (20) and the other with chain axes inclined ca. 60° to the methyl end plane as in the case of cetyl palmitate (21). Fourteen unique hk0 structure-factor magnitudes from the former polymorph (Table II) are found in agreement (R = 0.29) with the paraffin phasing model (22). Also 11 unique hk0 structure factor magnitudes from the tilted chain polymorph are correlated (Table III) with (R = 0.21) hk0 data from cetyl palmitate (23). Owing to the rarity of these polymorphs, they have not been characterized by crystal images.

Other Lipid Microcrystals

Microcrystals of DSPC, DPPC, DPPA, and NPGC all give hexagonal electron diffraction patterns with the characteristic spacing around 4.17 Å. Plastically deformed crystals grown around a screw dislocation, as well as dendrites, are seen with the galactocerebroside, NPGC (Fig. 8). The phosphatidic acid, DPPA, gives crystals grown around a screw dislocation with some evidence of a "turnover"-like fold (Fig. 9). Crystals of the phosphatidyl cholines DPPC and DSPC (Figs. 10 and 11) seem to favor a needle growth (see also Ref. 24) although screw dislocations are seen. Particularly salient here are outgrowths from the crystal surfaces.

Wet Lecithin Bilayers

A representative dark field electron micrograph from a torn wet bilayer of L-DPPC is shown in Fig. 12. The flexibility of the bilayer is apparent in the fold region near the tear. The acyl packing of these wet lecithin bilayers is again hexagonal with a (100) diffraction spacing at 4.20 Å (4). The electron diffraction intensity data are also well correlated with the rigid methylene rotor model (Fig. 2) used for the high temperature form of long chain lipids (4, 13, 17).

DISCUSSION

The data presented in this paper add weight to the argument that the more rotationally disordered (hexagonal) lipid chain packings produce greater flexibility in a biomembrane. A similar statement was made by Larsson (14), who found that a hexagonally packed thin film of glycerol-trioleate with a small amount of glycerol-l-monopalmitate impurity is very resilient to mechanical forces perpendicular to its surface. The normal

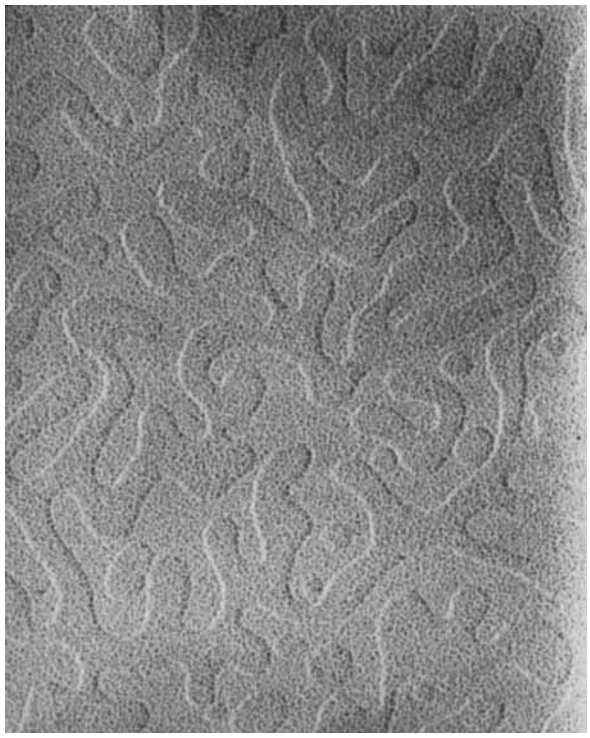

Fig. 5. Higher magnification of dendritic epitaxial overgrowth of type shown in Fig. 4.

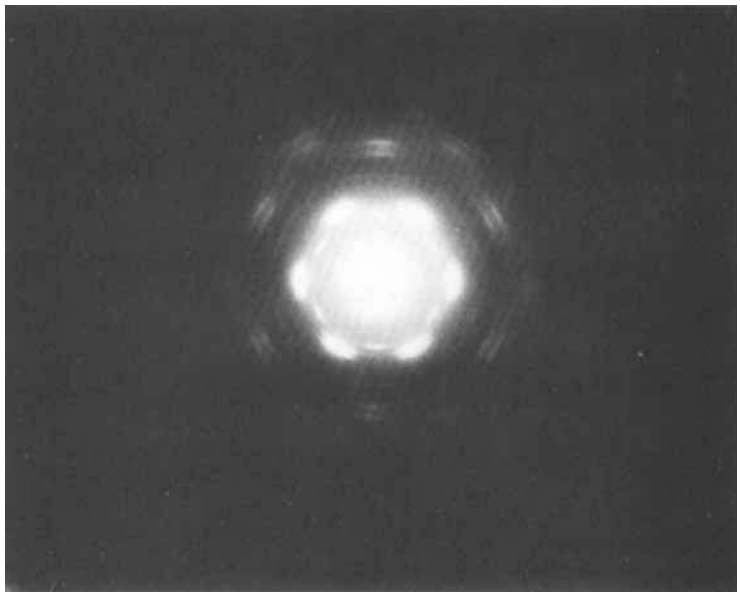

Fig. 6. Electron diffraction pattern from single crystal of sn-glycero-phosphoryl-ethanolamine, 1, 2-dihexadecyl ether using 14 μm diameter selected area.

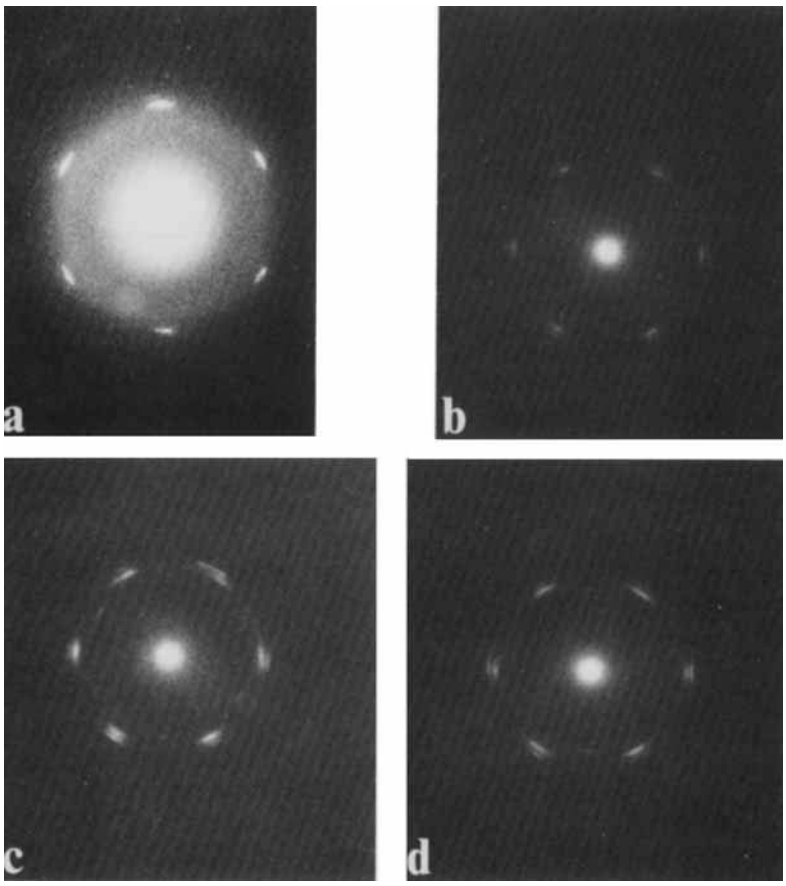

Fig. 7. Isolation of components in electron diffraction pattern of Fig. 6 by using smaller selected areas. (a) Hexagonal packing component (d_{100} = 4.17 Å). (b) Hexagonal packing component with hexagonally oriented overgrowth of orthorhombic component (d_{200} = 3.87 Å). (c) Hexagonal packing component and smeared contribution due to orthorhombic overgrowth. Note inner 4.68 Å hexad is present but that spots have unequal intensities. (d) Same as (c) except that 4.68 Å spots are no longer a hexad but a Friedel pair.

packing in biological membranes, indicated by the diffuse high-angle diffraction ring at around 4.6 Å (8, 10), is expected to be even more fluid than the rotationally disordered (hexagonal) chain packing considered here (although the 4.15 Å spacing is seen below the membrane lipid transition temperature [5]).

Apparently the more "crystalline" $0_{\perp}$ subcell gives less flexible lipid layers. As is shown in the diffraction contrast bright-field image of an orthorhombic n-hexatriacontane monolayer crystal (Fig. 13), contours indicating elastic bends up to 2° are often observed (Dorset, unpublished data). Yet more extreme forces on the surface (e.g., see Fig. 1 of Ref. 22) result in shears along [001]. Therefore, the more flexible hexagonal packing is preferable for biomembranes, although the lateral packing energy minimum is lower for the $0_{\perp}$ subcell than the hexagonal subcell (respective attractive potential energies: −1.99 kcal/molCH_2 vs. −1.78 kcal/mol CH_2) (25).

TABLE I. Structure Factor Magnitudes for Hexagonal Component of sn-Glycerol-Phosphoryl-Ethanolamine, 1, 2-Dihexadecyl Ether Electron-Diffraction Pattern

hk0	$\|F_{obs}\|$	F_{calc} (B = 4.0 Å^2)
100	9.5	+10.0
200	2.4	+2.2
110	3.7	+3.4

TABLE II. Structure Factor Magnitudes for $0_\perp$ Polymorph of sn-Glycerol-Phosphoryl-Ethanolamine, 1, 2-Dihexadecyl Ether*

hk0	$\|F_{obs}\|$	F_{calc} (B = 3.0 Å^2)	hk0	$\|F_{obs}\|$	F_{calc} (B = 3.0 Å^2)
200	4.61	6.79	020	3.48	4.15
400	3.04	3.12	120	1.62	−1.35
110	4.85	7.14	220	2.55	1.38
210	1.81	−1.48	320	2.35	−1.67
310	2.79	2.18	420	1.57	0.62
410	1.81	−1.19	130	2.25	2.14
510	1.27	1.21	230	2.06	−1.64

*a_s = 7.49 ± 0.04 Å; b_s = 5.00 ± 0.01 Å.

TABLE III. Structure Factor Magnitudes for $0_\perp$ Packing of sn-Glycerol-Phosphoryl-Ethanolamine, 1, 2-Dihexadecyl Ether, With ca. 30° Chain Tilt Around a_s, Compared to Similar Data From Cetyl Palmitate*

hk0	$\|F_o\|$ (DHPE)	$\|F_o\|$ (CP)	hk0	$\|F_o\|$ (DHPE)	$\|F_o\|$ (CP)
020	2.48	2.99	150	0.44	0.25
040	1.26	1.55	510	1.24	1.25
060	0.44	0.53	520	0	0
110	0.79	0.65	530	0.60	0.67
120	0.42	0.20	540	0	0
130	0.49	0.46	550	0.41	0.26
140	0.47	0.23			

*(See Ref. 22) a = 5.54 ± 0.03 Å, b = 7.17 ± 0.03 Å.

The epitaxial growth of other DHPE polymorphs on the underlying hexagonally packed crystal face is an interesting phenomenon. Such epitaxy is quite common for an interface of two materials, such as a metal oxide on its metal crystal surface, and can give diffraction patterns similar in appearance to Fig. 6 (26). To our knowledge, however, this is the first such observation on an isotropic medium. Since no superlattice can be drawn in Fig. 6 and since the diffraction pattern is shown in Fig. 7 to be composed of several components, we postulate that at least two (and maybe three) polymorphs of the phosphatidylethanolamine are growing on the hexagonally packed substrate layer. The major component, which accounts for the doubling of spots of the 4.17 Å hexagonal pattern (i.e., 3.87 Å), is probably composed of microcrystals of the $0_\perp$ subcell with chains normal to the surface, hexagonally disposed by epitaxy. Given that primary branches of cetyl palmitate dendrites (Dorset, unpublished data) bifurcate at an angle corresponding to the acute angle between {100} faces of the monoclinic polymorph (23), the observed 68°

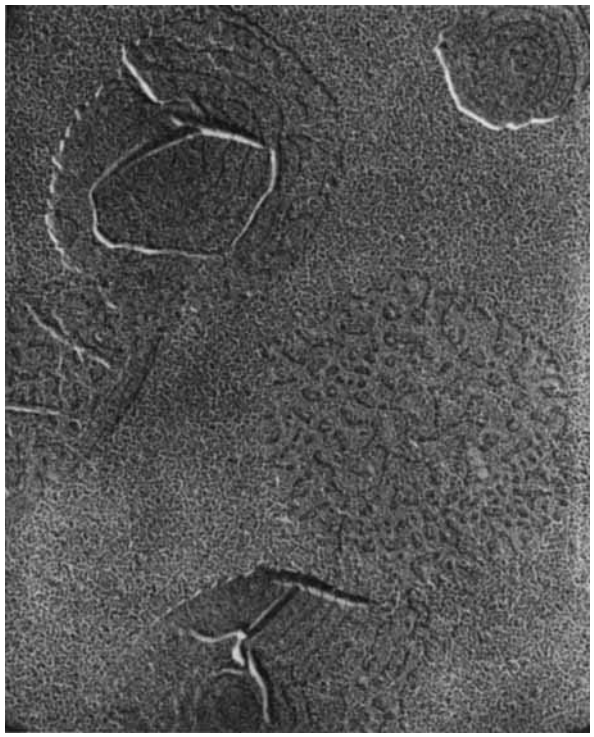

Fig. 8. Gold-shadowed crystals of N-palmitoyl dihydrogalactocerebroside showing both dendritic growths and fold-distorted growth around a screw disclocation.

branching of the dendritic overgrowth is in accord with the {110} interfacial angle for orthorhombic paraffins (22, 27) and supports the existence of this component. It is also easy to fit an $0_{\perp}$ (001) methyl end plane onto a hexagonal layer and to explain the three preferred epitaxial growth directions (Fig. 14). If an $0_{\perp}$ subcell of a = 7.49 Å and b = 5.00 Å epitaxially grows on a hexagonal substrate of a = 4.8 Å, the (110) spots of the former would almost superimpose on the (100) spots of the latter at a common spacing of 4.17 Å, whereas the (200) spots of the former would double the other hexagonal (100) spots at a spacing of 3.8 Å. Given an equal opportunity of growth along all three preferred directions, the composite diffraction pattern over a large area would show an apparent hexagonal symmetry (Fig. 6 and 7b). However, diffraction patterns selectively obtained from a few number of dendrites result in a breakdown of the hexagonal symmetry (Fig. 7c and d) as expected. The misfit of the overgrowth on the hexagonal substrate could also cause the arcing of the diffraction spots. The superposition of hexagonal and $0_{\perp}$ patterns have also been observed in multilayers (28) and "soap films" (4) of L-DPPC, indicating that the coexistence of two crystal habits of phospholipid is not uncommon.

The inner spacing at 4.68 Å is more difficult to explain. One possibility is a tilt of the aliphatic chains about the 5.00 Å $0_{\perp}$ subcell axis by about 38° to give a packing similar to the C-form of fatty acids (29). (A tilt of about 27° about the 7.49 Å $0_{\perp}$ subcell axis in another possible tilted polymorph would give a strong (020) reflection coincident with the (200) of the subcell and would not be discernible.) The alternate explana-

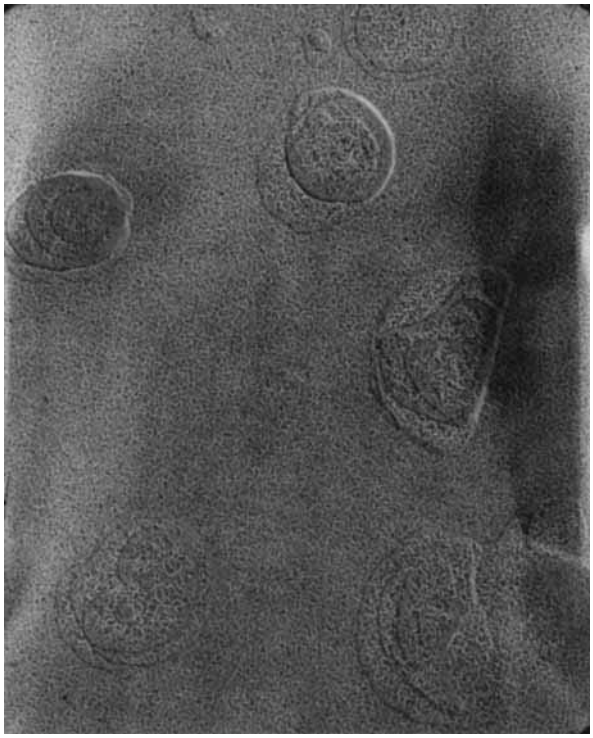

Fig. 9. Gold-shadowed crystals of 1, 2-dipalmitoyl-rac-glycerol phosphate showing growths around screw dislocation. Evidence of a "turnover"-type fold is seen for one crystal.

tion of the $T_{\parallel}$ subcell (30), which also has a strong (010) reflection at about 4.6 Å, is less likely because a strong $(\bar{1}10)$ reflection is expected at an azimuth of 50° from this reflection at 3.7 Å, and is not seen.

It is interesting to note in conclusion that folded or rolled crystals have also been observed for polymeric materials such as Nylon 66 grown from hot glycerine (31). The diffraction patterns at first glance seemingly contradict the data in this paper because the electron-diffraction patterns from the deformed crystals are due to the low temperature triclinic packing of the polyamide chains. A metastable high temperature hexagonal unit cell has been observed for Nylon 6, however, which is consistent with these observations of flexible lipid microcrystals, bilayers and membranes with disordered chain packing.

Fig. 10. Gold-shadowed crystals of 1, 2-dipalmitoyl-rac-glycerol phosphoryl choline showing outgrowths from surface.

Fig. 11. Gold-shadowed crystals of 1, 2-distearoyl-sn-glycerol phosphoryl choline showing outgrowths from surface.

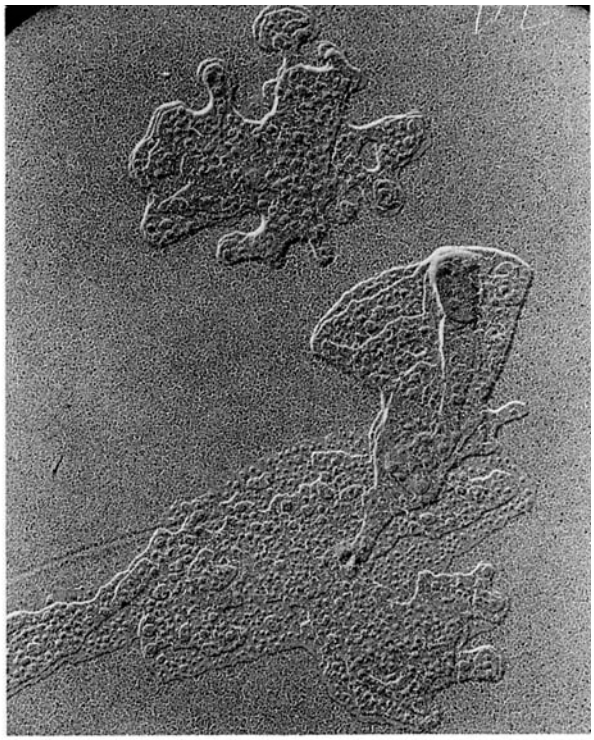

10

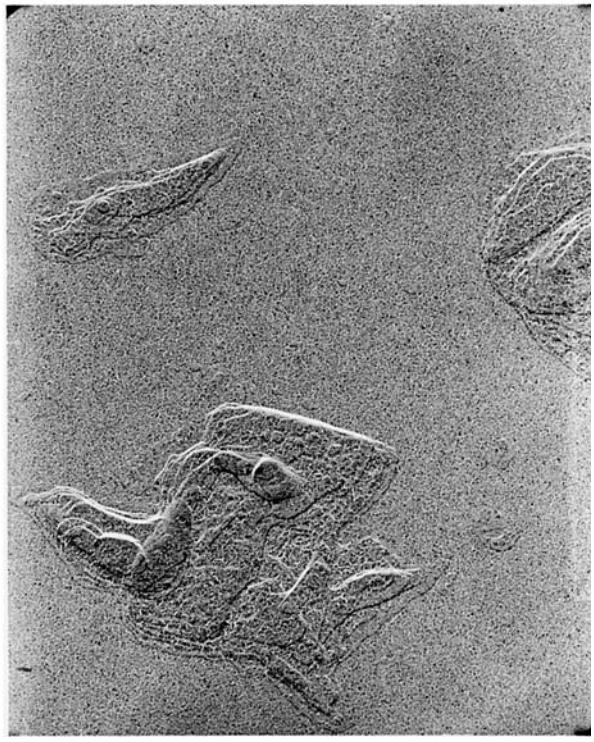

11

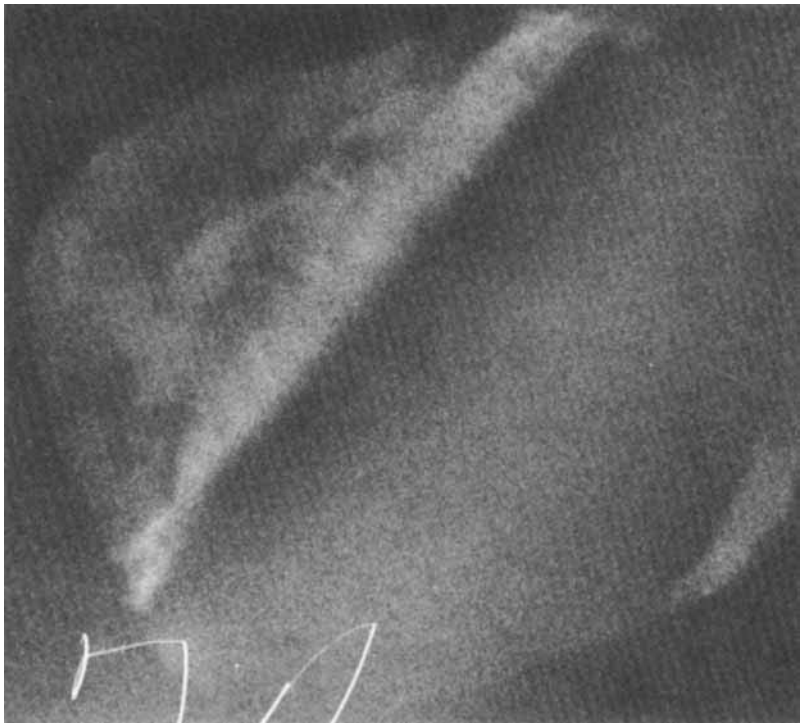

Fig. 12. Dark-field electron micrograph of a torn wet 1, 2-dipalmitoyl-sn-glycerol phosphoryl choline bilayer showing flexible folding of torn flap.

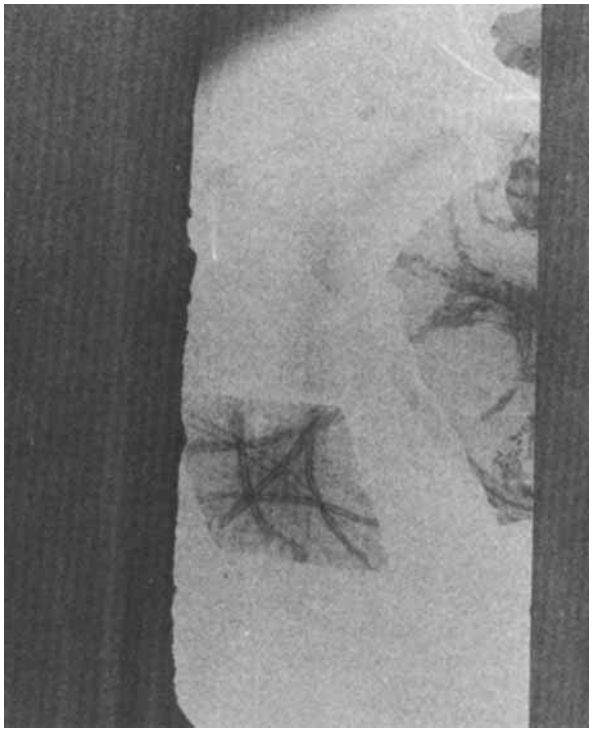

Fig. 13. Diffraction contrast bright-field electron image of n-hexatriacontane monolayer crystals showing bend contours corresponding to bend of $\simeq 2^{\circ}$.

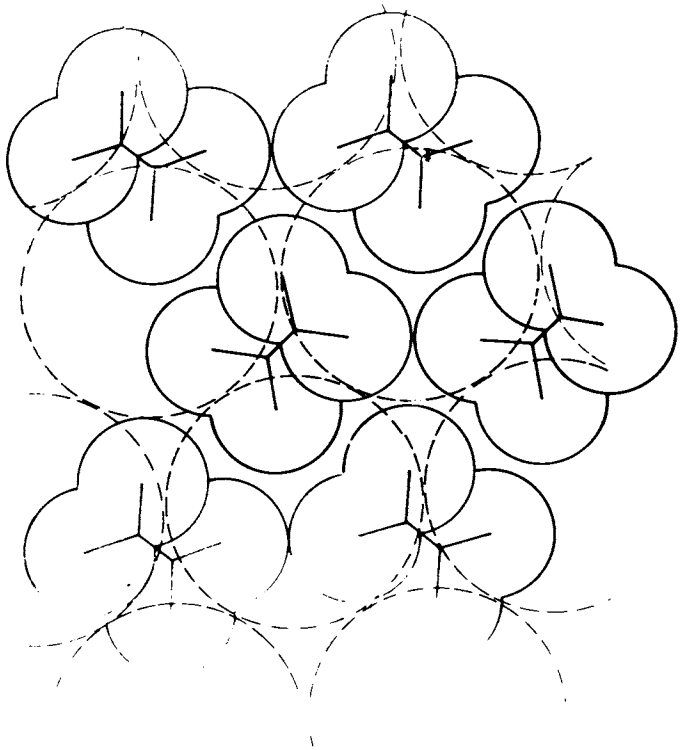

Fig. 14. Model for epitaxial growth of $0_{\perp}$ packed acyl chains on a hexagonally packed substrate. Although the fit of $0_{\perp}$ methyl projections into the holes defined by the hexagonal packing is not exact, the presence of distortions in the under layer, such as bending, could cause greater coincidence of the two layers. Alternatively, the possibility of an upper layer nucleated from an outgrowth of acyl chains crystallized in $0_{\perp}$ also exists, since in linear polymers this latter form of nucleation, and not the influence of end planes, dictates the crystal growth (32).

ACKNOWLEDGMENTS

Thanks are due to Dr. S. Ramalingam for permission to use the JEM-100U electron microscope in the Department of Mechanical Engineering, State University of New York at Buffalo. We also thank Mr. D. F. Harling for his courteous cooperation and assistance during our use of the JEM-100C electron microscope at JEOL USA, Inc., Medford, Mass. This research was supported by Public Health Service grants no. GM-21047 from the National Institute of General Medical Sciences and no. CA-15330 from the National Cancer Institute. S.W.H. acknowledges support from NIH Career Development Award CA-00084.

REFERENCES

1. Hurst, H., J. Exp. Biol. 27:238–252 (1950).
2. Hurst, H., J. Exp. Biol. 29:30–53 (1952).
3. Carlemalm, E., and Wieslander, Å., Nature 254:537–538 (1975).
4. Hui, S. W., Parsons, D. F., and Cowden, M., Proc. Nat. Acad. Sci. (USA) 71:5068–5072 (1974).
5. Hui, S. W., and Parsons, D. F., Science 184:77–78 (1974).
6. Hui, S. W., Parsons, D. F., and Cowden, M., Proc. 32nd Ann. Electr. Microsc. Soc. America Meeting, Claitor's Publ. Div., Baton Rouge, pp. 160–161 (1974).

7. Hui, S. W., Cowden, M., Papahadjopoulos, D., and Parsons, D. F., Biochim. Biophys. Acta 382:265–275 (1975).
8. Hui, S. W., and Parsons, D. F., Proc. 32nd Ann. Electr. Microsc. Soc. America Meeting, Claitor's Publ. Div., Baton Rouge, pp. 158–159 (1974).
9. Hui, S. W., and Parsons, D. F., In "Advanced Techniques in Biological Electron Microscopy" J. K. Koehler, (Ed.), vol. 2 (in press).
10. Levine, Y. K., Progr. Biophys. Molec. Biol. 24:1–74 (1972).
11. Hitchcock, P. B., Mason, T., Thomas, K. M., and Shipley, G. G., Proc. Nat. Acad. Sci. (USA) 71:3036–3040 (1974).
12. Dorset, D. L., Biochim. Biophys. Acta 424:396–403 (1976).
13. Dorset, D. L., Biochim. Biophys. Acta 380:257–263 (1975).
14. Larsson, K., Chem. Phys. Lipids 14:233–235 (1975).
15. Gitler, C., Ann. Rev. Biophys. Bioeng. 1:51–92 (1972).
16. Papahadjopoulos, D., Jacobson, K., Nir, S., and Isac, T., Biochim. Biophys. Acta 311:330–348 (1973).
17. Dorset, D. L., Chem. Phys. Lipids 13:133–140 (1974).
18. Hui, S. W., Hausner, G. G., and Parsons, D. F., J. Phys. E. 9:69–72 (1975).
19. Larsson, K., Nature 213:383–384 (1967).
20. Teare, K., Acta Crystallogr. 12:294–300 (1959).
21. Kohlhaas, R., Z. Krist. 98:418–438 (1938).
22. Dorset, D. L., Acta Crystallogr. A32:207–216 (1976).
23. Dorset, D. L., Bioorg. Khim. (in press).
24. Dorset, D. L., Naturwissenschaften 62:343–344 (1975).
25. Ploc, R. A., J. Nucl. Mater. 28:48–60 (1968).
27. Amelinckx, A., Acta Crystallogr. 9:217–224 (1956).
28. Hui, S. W., Chem. Phys. Lipids 16:9–18 (1976).
29. Malta, V., Celotti, G., Zannetti, R., and Martelli, A. F., J. Chem. Soc. (B):548–553 (1971).
30. Vand, V., and Bell, I. P., Acta Crystallogr. 4:465–469 (1951).
31. Geil, P. H., J. Polym. Sci. 44:449–457 (1960).
32. Geil, P. H., in "Polymer Single Crystals," John Wiley & Sons, Inc., New York p. 101 ff, (1963).
33. Vainshtein, B. K., Sov. Phys.-Crystallogr. 8:127–130 (1963).